11-2016

Autonomous Navigation and Hazard Evasion Platform for Personal UAV's

Ryan Scott

Portland State University

Autonomous Navigation and Hazard Evasion Platform for Personal UAV's

An undergraduate honors thesis submitted in partial fulfillment of the requirements for the degree of Bachelor of Science in University Honors and Mechanical Engineering.

Ryan Scott
Portland State University 2016

Thesis Advisor:
Dr. Nathalie Neve

Abstract

Personal UAV's are experiencing an increase in both functionality and popularity. Consumer-driven markets are encouraging the UAV industry to innovate towards the average user. Despite improvements in user friendliness, cost, and technological capabilities, consumer UAV's are limited by pilot skill and a lack of sensory information. This paper presents two approaches for creating a low-cost, open-source platform capable of enabling a consumer-level UAV to avoid hazards. A single beam LIDAR system and a combined LIDAR-vision system are considered. The LIDAR variant is capable of detecting and avoiding static obstacles in simple environments. The improved LIDAR-vision system is able to detect and avoid moving hazards in complex environments such as a bike path with pedestrian foot traffic. Finally a unified system with improved hardware capabilities is proposed.

Contents

1 Abstract

Personal UAV's are experiencing an increase in both functionality and popularity. Consumer-driven markets are encouraging the UAV industry to innovate towards the average user. Despite improvements in user friendliness, cost, and technological capabilities, consumer UAV's are limited by pilot skill and a lack of sensory information. This paper presents two approaches for creating a low-cost, open-source platform capable of enabling a consumer-level UAV to avoid hazards. A single beam LIDAR system and a combined LIDAR-vision system are considered. The LIDAR variant is capable of detecting and avoiding static obstacles in simple environments. The improved LIDAR-vision system is able to detect and avoid moving hazards in complex environments such as a bike path with pedestrian foot traffic. Finally a unified system with improved hardware capabilities is proposed.

2 Introduction

The consumer UAV (Unmanned Areal Vehicle) market is expected to quadruple within the next five years as the capabilities of personal UAV's continue to develop and the industry expands to encompass new consumer bases [1]. Despite government regulations, consumer UAV's are finding applications in diverse areas such as land management, photography, film, and construction [1][2]. Innovations in UAV technology like geo-fencing, autonomous navigation, and collision avoidance have lowered the threshold for operating personal UAV's [1]. Ease of piloting and decreasing ownership costs appeal to casual enthusiasts who now comprise a significant portion of the private (non-defense) UAV market [2]. Shifts in customer base from professionals to new consumers combined with technological advancements have stimulated industry development towards creating airborne smartphone-like media platforms. These UAV's are generalized as having a camera, wireless connectivity, a user-friendly interface, and an on-board flight controller. Common designs for a consumer grade UAV are the quadcopter, named for having four rotors in an 'X'configuration (Figure 1a), its cousin the hexacopter which has six rotors equidistant from its center (Figure 1b), and the octocopter style with eight equally spaced rotors (Figure 1c). Despite recent advances in navigation technology, quadcopters rely primarily on pilot skill for traversing complex environments. Evading hazards and performing similarly difficult navigation tasks pose a danger for bystanders and the UAV itself due to the high likelihood of a collision. Enabling UAV's to adapt to their surroundings by sensing and avoiding obstacles has been the focus of both scholarship and industrial research [1][2]. As such, a variety of sensor driven techniques now exist to resolve this issue. Depth sensors including laser scanners and sonar have been deployed in numerous configurations [3][4][5]. Vision guided systems have gained popularity as small onboard flight computers and companion computers have increased in power. Multi-camera systems have simulated depth information from stereoscopic vision [6] while single camera platforms have been used to inform probabilistic motion models [7][8]. Integrating sensor and vision systems has produced structured light devices capable of digitally recreating a 3D environment such as the Xbox Kinect [9] and Intel RealSense [10]. At the consumer level, hazard evasion platforms are beholden to weight, cost, and power consumption restrictions to a greater degree than large UAV's. For instance, the Xbox Kinect is physically too large

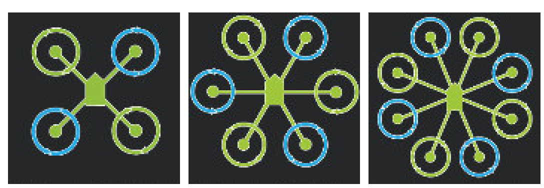

(a) Quadcopter layout (b) Hexacopter layout (c) Octocopter layout

Figure 1: Three popular personal UAV layouts in the multirotor family.

to be carried by consumer grade UAV's. Laser and sonar systems are similarly limited by size and power constraints, often reducing them to single beam range finders. As sensor packages are compromised to reduce cost, they decrease in functionality to the point of becoming nonviable for providing the detailed information required for maneuvering in complex 3D environments. Vision based systems and structured light devices have been more readily scaled and adopted by the consumer UAV industry. Currently, the DJI Mavic [11], Yuneec Typhoon H [10], and AscTec Firefly [12] are the first commercially available quadcopters with hazard detection and advanced GPS assisted flight paths. UAV manufacturer Parrot has announced an aftermarket sensor package for some of its products [13]. The Typhoon H and Firefly both rely entirely on Intel RealSense structured light sensors for situational awareness and straddle the boundary between consumer and professional pricing with the Firefly being the more expensive of the two [10][12]. Both the DJI Mavic and Parrot sensor package have yet to be released but boast multi-sensor integration for enhanced navigation and obstacle avoidance [11][13]. Although the consumer UAV industry is focusing on multi-sensor integration [2], the potential for a low cost, open-source, universal hazard evasion platform has yet to be well investigated. This paper analyzes two distinct methodologies for addressing the present disconnect between performance, cost, and transparency with the goal of obtaining high-level functionality from low cost consumer UAV's. Distance sensor and combined vision-sensor platforms are considered and tested in the context of detecting obstacles for the purpose of real-time evasion by a consumer grade UAV.

3 Materials and Methods

3.1 Prototype One: LIDAR Based Hazard Detection and Evasion

3.1.1 Hardware

LIDAR distance sensors were chosen to detect hazards in front of the vehicle (3D Robotics 2014 DIY Quadcopter [14], 3D Robotics 2015 SOLO Quadcopter [15]). A microcontroller (Arduino Uno R3 [16]) was responsible for translating LIDAR measurements into navigation commands for the vehicle's autopilot (Pixhawk, Pixhawk 2 [17]). Low cost, single beam LIDAR sensors (LIDAR-Lite V1, V2[18]) were directed into a rotating mirror at a rate of 750 readings per second to create a planar arc of range measurements (Figure 2). The mirror was mounted vertically on a high-speed servomotor (Turnigy TGY-50090M) in a 3D printed enclosure (Figure 3). A WAAS GPS unit (Xbee) was chosen to provide constant ground reference coordinates at a rate of once per second for navigation. Power management on the quadcopter was handled by the microcontroller which was connected to one of the autopilot's auxiliary power ports. The GPS device was powered from a 9V battery.

3.1.2 GPS Navigation

A Dronekit [19] GOTO command was issued to the vehicle each second directing it to the ground reference GPS coordinates during operation. The heading was such that the vehicle was assumed to always face the direction of the GPS ground reference.

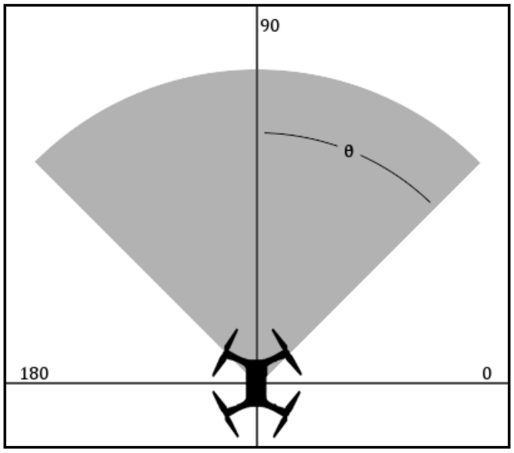

Figure 2: LIDAR scanning pattern where θ represents scan angle relative to the vehicle. 90°is assumed to orient towards the GPS ground reference.

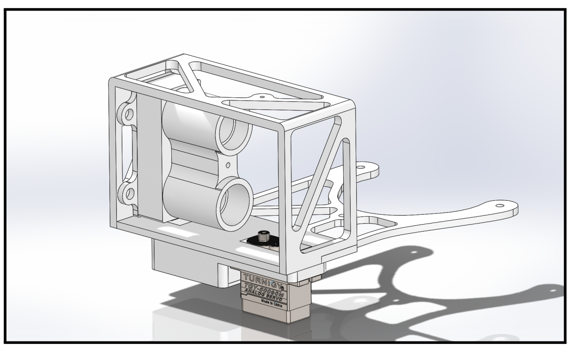

Figure 3: 3D CAD model of the LIDAR unit mounted in a custom enclosure with the rotating mirror and servo motor.

3.1.3 Point Cloud Generation

Upon detecting an object closer than the safety trigger value (30m) with the forward facing LIDAR, an arc of distance measurements was acquired. The LIDAR scanned through each value of theta for angles between 45 and 135 degrees at an increment of 1 degree per measurement in a sweeping pattern. Two sets of measurements were created per scan: one for theta between 45 and 135 degrees and one for returning angles between 135 and 45 degrees. To account for the forward motion of the vehicle during scanning, measurements sharing the same angle were averaged. Averaging was implemented to minimize the potential differences in distance values stemming from time elapsing between a distance readings, ensure values of theta were not overrepresented, and reduce the chance of a faulty measurement showing an obstacle where none were present.

3.1.4 Data Interpretation and Navigation

The resulting average distances were compared by recording the number of consecutive distance measurements above the trigger value. Each measurement above 30m and the corresponding angle were added to an array. An array of measurements was considered ”safe” if it contained greater than eight uninterrupted measurements greater than 30 m. The center of the largest ”safe” arc in the direction of the GPS ground reference was chosen and a left/right roll command proportional to the theta value for the center of the ”safe” arc was sent to the vehicle's autopilot (Figure 4).

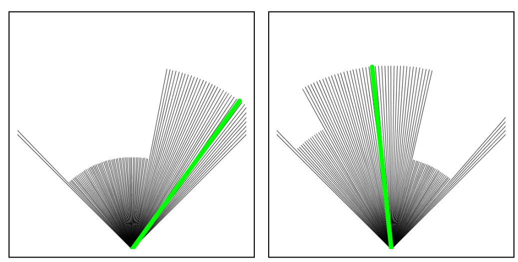

(a) Scan with one obstacle.

(b) Scan with two obstacles present.

Figure 4: Two test scans with the LIDAR system. Gaps in coverage reveal the location of obstacles and large green lines show the projected evasion flight path.

3.2 Prototype 2: Hazard Detection and Evasion Through Image Processing

3.2.1 Hardware

A 5MP digital camera (Raspberry Pi Camera Module V1 [20]) was connected to a single board computer (Raspberry Pi 2 Model B [21]) to process images in front of the vehicle (3D Robotics 2015 SOLO Quadcopter). The Raspberry Pi was integrated with the vehicle's autopilot through its local WIFI network. One single-beam LIDAR range sensor (LIDAR-Lite V2) was mounted directly above the camera on a 3D printed enclosure (Figure 5). The LIDAR unit collected distance measurements at a rate of 750 readings per second and the camera captured still images at a rate of 90 frames per second. Power for the system passed through the 24V accessory rail into a DC-DC converter to provide stable 5V power at 1A to the Raspberry Pi.

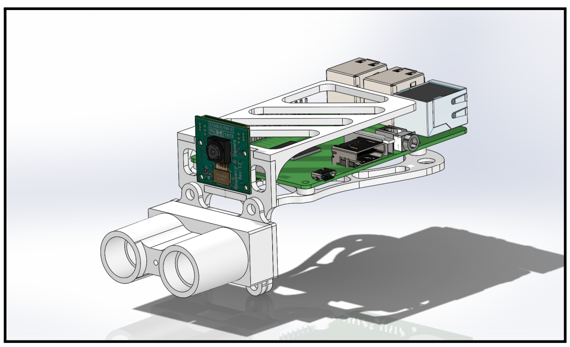

Figure 5: Updated CAD model of the LIDAR unit and color camera mounted with the Raspberry Pi 2 in a custom enclosure.

3.3 Navigation

The vehicle came equipped with GPS navigation and tracking. Further development of WAAS GPS navigation using the ground reference unit was halted.

3.3.1 Image Acquisition and Processing

Images and distance measurements were taken continuously from the time of liftoff to avoid hardware startup lag during operational flight. Image capture and processing were split between two parallel threads on the Raspberry Pi. When an obstacle in front of the quadcopter closer than the safety threshold distance (30m) was detected by the LIDAR, a set of twenty consecutive images were pulled from the continuous capture thread into the image processing thread (Figure 6a). Each new capture was compared to previous images to determine pixel motion using a K-nearest neighbors background subtraction algorithm. Change in pixel motion was used to provide an estimate of object persistence between images. The algorithm presented pixel translation between frames with a gradient fluctuating between 0 and 255 where pixels with significant movement were assigned higher values (Figure 6b) Objects detected by pixel motion across multiple images were assumed to have a velocity relative to the quadcopter and present a risk of collision. Objects very far from the camera, such as the sky, would not appear to move between images while objects very close to the camera with the highest risk of collision would consistently have large translations. The complete set of still images was averaged to create a single array representing motion where larger values indicated consistent motion relative to the vehicle; which was then inverted (Figure 6c) The vehicle's current velocity and heading were simultaneously logged in a third parallel thread.

(a) Example of an original image.

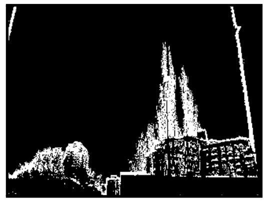

(b) Image after applying the background subtraction algorithm.

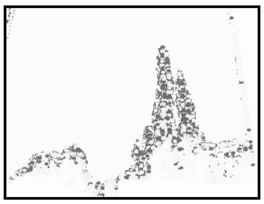

(c) Composite image made of the average of twenty consecutive pixel motion images prior to inverting. Darker areas indicate persistent motion between frames. The trees are consistently detected at any distance because of the constant motion of their leaves. Buildings and similarly stationary objects must be closer to the camera before they are similarly represented.

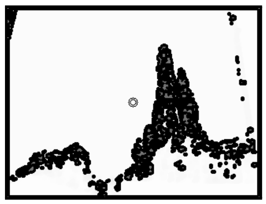

(d) Final image with the coordinates of the safe area marked by two concentric circles. The coordinates represent the navigation destination's location on the image plane and are provided to visually confirm the safe area is in a valid location.

Figure 6: Image processing pipeline.

3.3.2 Data Interpretation and Navigation

The trigger distance and vehicle velocity were used to estimate the time until impact with the trigger object. This information was also used to estimate the size of the vehicle on the image plane at the time of impact. Topological border detection was performed on the inverted motion sum image to locate "safe" areas. An area in the image plane was considered "safe" if it was larger than the estimated size of the vehicle multiplied by a factor of safety (2.0). The closest "safe" area to the center of the picture along the vehicle's current heading was chosen (Figure 6d) Final image. Left/right roll and raise/lower commands were sent to the autopilot based on the quadcopter's velocity components and heading at the time of hazard detection and the location of the "safe" area.

4 Results and Discussion

4.1 Prototype One: LIDAR Based Hazard Detection and Evasion

The LIDAR system performed at a rate of approximately one second from detecting a hazard to sending a navigation command when operating with LIDAR-Lite V2. The first generation of LIDAR-Lite was at least five seconds slower per flight command and deemed unsuitable for UAV navigation early in its testing cycle. The final system was capable of avoiding multiple large stationary obstacles in simple environments such as a chair and table in large room. The system was capable of operating at the UAV's maximum quoted airspeed of 15 m/s and had a final cost of $ 130 for the LIDAR-Lite V2, Arduino UNO, and Servo Motor.

Several limitations were present which resulted in the decision to move to an image-based platform. An obstacle's surface characteristics, such as opacity and reflectivity, were constant failure mechanisms for the LIDAR unit. This is because LIDAR beam was incapable of correctly returning to its receiver after interacting with these surfaces. Translucent surfaces created internal reflection and partial beam refraction rather than total reflection causing the sensor's timer to lapse, resulting in a seized unit with LIDAR-Lite V1 and non-numeric values from LIDAR-Lite V2. Additional deficiencies were inherited from the scanning pattern. Regular gaps between measurements were present beyond a certain distance and the system had to be perfectly level to properly scan for obstacles. The laser's aperture diameter was 12mm wide by 2mm high with a divergence of 4 mRadian by 2 mRadian. Therefore, when scanning, continuous horizontal coverage was only possible at distances closer than 0.89 m. At the maximum range of 40 m, gaps as in coverage as large as 0.52 m were possible. As noted previously, if the quadcopter was not level to the horizon when scanning, the point cloud would erroneously classify the ground as an obstacle resulting in invalid flight commands.

4.2 Prototype 2: Hazard Detection and Evasion Through Image Processing

The image-based system was capable of sending a flight command within two and a half seconds of detecting an object using multi-threading and a LIDAR-Lite V2 unit. This system was capable of avoiding both stationary and moving obstacles in complex environments such as trees with moving pedestrians on a bike path. The flight commands were independent of whether or not the quadcopter was level while scanning and coverage was unbroken within the visible range of the camera. The system limited the UAV's safe nominal airspeed to 10 m/s and had a final cost of $ 155 for the LIDAR unit, Raspberry Pi V2, and Raspberry Pi camera module V1. The complete system is depicted in Figure 7.

Performance of the LIDAR-vision system was limited by a variety of hardware and software factors. The LIDAR-Lite unit suffered from the same inability to properly detect reflective or transparent surfaces present in the previous system. The camera required ample light for operation, reducing the usefulness of the system to daylight hours. In addition, the rate at which images could be processed after acquisition and their definition were hampered by the hardware capabilities of the Raspberry Pi. In order to increase processing speed, image resolution was reduced to the lowest possible level while retaining the ability to distinguish objects of similar pixel size to the quadcopter. Parallel threads were utilized to allow an entire core for performing the K-nearest neighbors background subtraction in a further effort to optimize operation speed. The main failure mechanism developed from a fault in the topological border detection algorithm. The algorithm failed when objects lacked clearly defined boundaries. Overlapping objects of similar colors, similar values, and blurry objects were potential sources for noncontinuous boundaries. When the algorithm failed to detect closed boundaries, it would return an empty array which prevented further processes from having access to any location information. As the number of obstacles in an image increased, the likelihood of hazards overlapping or neighbors sharing visual characteristics increased which in turn increased the likelihood of the border detection failing. Noise removal and feature grouping were both explored as possible solutions to artificially insulate the border detection algorithm from open contours. However, neither was capable of resolving the breakdown without imposing issues of their own. Feature grouping resulted in the complete loss of some obstacles due to image homogenization removing the obstacle's borders entirely. Noise removal was more successful but decreased the platforms sensitivity to a point at which hazards such as power lines and street signs were no longer visible until they were too

Figure 7: Final system mounted on the 3D Robotics SOLO during testing field.

close to avoid.

4.3 Conclusions

The LIDAR-vision system outperformed the LIDAR system with regard to detecting the multitude of obstacles encountered by a consumer UAV. It succeeded in detecting both stationary and mobile hazards within the visible range of the camera whereas the LIDAR system was prone to gaps in coverage, misidentification, and was limited to one plane. Yet, the LIDAR system was less expensive, independent of lighting conditions, and produced a flight command on average one and a half seconds more quickly. Overall, the LIDAR-vision system was determined to be more practical for UAV hazard evasion for its ability to detect both stationary and moving obstacles in 3D space and provide 3D rather than planar navigation.

4.4 Future Work

Further progress on the LIDAR system would be possible if a two-axis gimbal capable of maintaining a horizontal scanning field were used in conjunction with an upgraded LIDAR sensor. Such a system would require maintaining a level relation to the ground and increasing either the number of LIDAR measurements or the rate at which measurements are acquired. Many recent camera gimbals include leveling functionality so including a small scanning module on an existing camera setup is possible. To obtain more data points, a higher speed motor for mirror rotation or a higher performance LIDAR unit are both possible solutions. Another method for eliminating measurement gaps with the existing system is to modify the beam characteristics to produce wider beam and recalibrate the unit.

The LIDAR-system system could be improved in a number of areas. A more powerful processor could potentially handle more complex environments by processing higher resolution images. It could also reduce the amount of time between detecting an object and sending a flight command. A more robust optical flow algorithm could greatly improve number of objects the system detects and their relative locations. A superior border detection algorithm is the most pressing area for evolving the LIDAR-vision system. The next step in this area would likely involve writing a custom optical flow and border detection algorithm to meet the specific needs of high speed and low sensitivity to discontinuity. An ideal system would utilize the advantages of both methods to rapidly provide overlapping levels of sensory information to the flight computer.

References

[1] J. Camhi, "THE DRONES REPORT: Market forecasts, regulatory barriers, top vendors, and leading commercial applications," Business Insider, Market Analysis, Jun. 2016. [Online]. Available: http://www.businessinsider.com/uav-or-commercial-drone-market-forecast-2015-2

[2] G. V. Research, "Consumer Drone Market Analysis By Product (Multi-Rotor, Nano), By Application (Prosumer, Toy/Hobbyist, Photogrammetry) And Segment Forecasts To 2024," Grand View Research, Market Analysis 2024, 2016. [Online]. Available: http://www.grandviewresearch.com/industry-analysis/consumer-drone-market

[3] A. Wehr and U. Lohr, "Airborne laser scanning—an introduction and overview," *ISPRS Journal of Photogrammetry and Remote Sensing*, vol. 54, no. 2–3, pp. 68–82, Jul. 1999. [Online]. Available: http://www.sciencedirect.com/science/article/pii/S0924271699000118

[4] E. N. Johnson, J. G. Mooney, C. Ong, V. Sahasrabudhe, and J. Hartman, "Flight testing of nap of-the-earth unmanned helicopter systems," *Georgia Tech Library*, May 2011. [Online]. Available: https://smartech.gatech.edu/handle/1853/46843

[5] B. Schwarz, "Mapping the World in 3d," Nature Photonics, Technology Overview 4, Jul. 2010.

[6] A. J. Barry and R. Tedrake, "Pushbroom Stereo for High-Speed Navigation in Cluttered Environments," *arXiv:1407.7091 [cs]*, Jul. 2014, arXiv: 1407.7091. [Online]. Available: http://arxiv.org/abs/1407.7091

[7] Y. Watanabe, A. Calise, and E. Johnson, "Vision-Based Obstacle Avoidance for UAVs," in *AIAA Guidance, Navigation and Control Conference and Exhibit*. American Institute of Aeronautics and Astronautics, aug 2007. [Online]. Available: http://arc.aiaa.org/doi/abs/10.2514/6.2007-6829

[8] D. Magree, J. G. Mooney, and E. N. Johnson, "Monocular Visual Mapping for Obstacle Avoidance on UAVs," *Journal of Intelligent & Robotic Systems*, vol. 74, no. 1-2, pp. 17–26, Oct. 2013. [Online]. Available: http://link.springer.com/article/10.1007/s10846-013-9967-7

[9] J. Stowers, M. Hayes, and A. Bainbridge-Smith, "Altitude control of a quadrotor helicopter using depth map from Microsoft Kinect sensor," in *2011 IEEE International Conference on Mechatronics (ICM)*, Apr. 2011, pp. 358–362.

[10] Yuneec, "Intel® RealSense™ Technology." [Online]. Available: http://yuneec.com

[11] DJI, "Mavic - Wherever you go." [Online]. Available: http://www.dji.com/mavic

[12] AscTec, "AscTec Firefly - AscTec Research - Ascending Technologies Customer Wiki." [Online]. Available: http://wiki.asctec.de/display/AR/AscTec+Firefly

[13] Parrot, "Parrot S.L.A.M. Dunk," Sep. 2016. [Online]. Available: https://corporate.parrot.com/en/pressrelease/parrots.l.a.m.dunkturnadroneintoasmartrobot

[14] D. Robotics, "DIY QUAD," 2014. [Online]. Available: https://3dr.com/wp-content/uploads/2014/05/3DR-DIY-Quad-Build-Manual-vA.pdf

[15] ——, “Introduction | 3dr Solo Development Guide.” [Online]. Available: http://dev.3dr.com/

[16] Arduino, “Arduino uno.” [Online]. Available: https://www.arduino.cc/en/Main/ArduinoBoardUno

[17] P. Project, “Home - Pixhawk Flight Controller Hardware Project.” [Online]. Available: https://pixhawk.org/

[18] P. Light, “PulsedLight3d/LIDAR-Lite-Documentation.” [Online]. Available: https://github.com/PulsedLight3D/LIDAR-Lite-Documentation

[19] D. Robotics, “Welcome to DroneKit-Python’s documentation!” [Online]. Available: http://python.dronekit.io/

[20] D. Jones, “picamera — Picamera 1.10 documentation.” [Online]. Available: http://picamera.readthedocs.io/en/release-1.10/

[21] R. Kinch, “Information and Products for Custom Applications and Engineering.” [Online]. Available: http://www.truetex.com/raspberrypi